

Assessment of metal artifacts in three-dimensional dental surface models derived by cone-beam computed tomography

Wael Nabha^a
Young-Min Hong^a
Jin-Hyoung Cho^b
Hyeon-Shik Hwang^b

^aDepartment of Orthodontics, School of Dentistry, Chonnam National University, Gwangju, Korea

^bDepartment of Orthodontics, School of Dentistry, Dental Science Research Institute, Chonnam National University, Gwangju, Korea

Objective: The aim of this study was to assess artifacts induced by metallic restorations in three-dimensional (3D) dental surface models derived by cone-beam computed tomography (CBCT). **Methods:** Fifteen specimens, each with four extracted human premolars and molars embedded in a plaster block, were scanned by CBCT before and after the cavitated second premolars were restored with dental amalgam. Five consecutive surface models of each specimen were created according to increasing restoration size: no restoration (control) and small occlusal, large occlusal, disto-occlusal, and mesio-occluso-distal restorations. After registering each restored model with the control model, maximum linear discrepancy, area, and intensity of the artifacts were measured and compared. **Results:** Artifacts developed mostly on the buccal and lingual surfaces. They occurred not only on the second premolar but also on the first premolar and first molar. The parametric values increased significantly with increasing restoration size. **Conclusions:** Metallic restorations induce considerable artifacts in 3D dental surface models. Artifact reduction should be taken into consideration for a proper diagnosis and treatment planning when using 3D surface model derived by CBCT in dentofacial deformity patients. [Korean J Orthod 2014;44(5):229-235]

Key words: Cone-beam computed tomography, Three-dimensional surface model, Artifact, Metallic restoration

Received February 1, 2014; Revised March 17, 2014; Accepted March 18, 2014.

Corresponding author: Hyeon-Shik Hwang.

Professor and Chairman, Department of Orthodontics, School of Dentistry, Chonnam National University, Yongbong-ro 33, Buk-gu, Gwangju 500-757, Korea.

Tel +82-62-530-5841 **e-mail** hhwang@chonnam.ac.kr

*This research was supported by Basic Science Research Program through the National Research Foundation of Korea (NRF) funded by the Ministry of Education (NRF-2010-0025828).

The authors report no commercial, proprietary, or financial interest in the products or companies described in this article.

© 2014 The Korean Association of Orthodontists.

This is an Open Access article distributed under the terms of the Creative Commons Attribution Non-Commercial License (<http://creativecommons.org/licenses/by-nc/3.0>) which permits unrestricted non-commercial use, distribution, and reproduction in any medium, provided the original work is properly cited.

INTRODUCTION

Three-dimensional (3D) computed tomography (CT) provides accurate and detailed information for diagnosis and treatment planning of dentofacial deformities. Although volume-rendered and multiplanar reconstructed images are mostly used, 3D surface models are more useful in some circumstances, such as evaluation of facial asymmetry^{1,2} and computer-assisted surgical simulation.³⁻⁶

Despite the many advantages of 3D CT, detailed occlusal and accurate interocclusal data cannot be obtained. Moreover, image quality is affected by artifacts induced by various factors such as beam hardening, extinction, scatter, noise, exponential edge gradient effect, aliasing, partial volume effect, and object motion.⁷⁻¹⁰ In particular, the quality is worsened by the existence of metals such as orthodontic brackets and dental restorations.^{7,11,12}

To overcome this limitation, attempts have been made to combine maxillofacial CT images with digital dental models.¹³⁻¹⁸ In this method, the dental part of a CT image is replaced with a 3D dental surface model created by optical¹⁴ or laser scanning.^{13,15-18} Nevertheless, artifacts influence image accuracy when surface registration is used for the fusion.^{14,18} The purpose of this study was to assess artifacts induced by metallic restorations in 3D dental surface models derived by cone-beam computed tomography (CBCT).

MATERIALS AND METHODS

For this study, extracted human premolars and molars were prepared by removing soft tissue, residual

bone, and calculus and embedded in plaster blocks (15 specimens with four different teeth per specimen) such that their crowns were aligned as in the natural dentition. In each specimen, cavities of increasing size were prepared in the second premolar according to the standard methods¹⁹ and the tooth was restored with dental amalgam, as follows: no restoration (control), small occlusal restoration, large occlusal restoration, disto-occlusal restoration, and mesio-occluso-distal restoration (Figure 1). Five sequential scans were obtained with a CBCT scanner (Alphard Vega; Asahi Roentgen Ind. Co., Kyoto, Japan) before and after the restorations under the following conditions: 80 kV, 5 mA, 0.39 × 0.39 × 0.39 mm voxel size, and 200 × 179 mm field of view (FOV). The images were saved in Digital Imaging and Communication in Medicine (DICOM) format and imported into imaging software (InVivoDental 5.0; Anatomage, San Jose, CA, USA). Then, 3D surface models were constructed by using segmentation threshold values ranging from 600 to 3,071 according to the program's default function and converted to stereolithographic format.

To reveal artifacts, each restored model was registered with the control model by using the iterative closest point algorithm²⁰ in 3D reverse engineering software (Rapidform 2006; INUS, Seoul, Korea). The initial registration was performed by selecting three corresponding points on both models. Regional registration was used to calculate rotation and translation from surface information of the two data sets. Corresponding points and shapes were searched and their distance was minimized after rotation and translation. Discrepancies between the models were shown by color mapping.

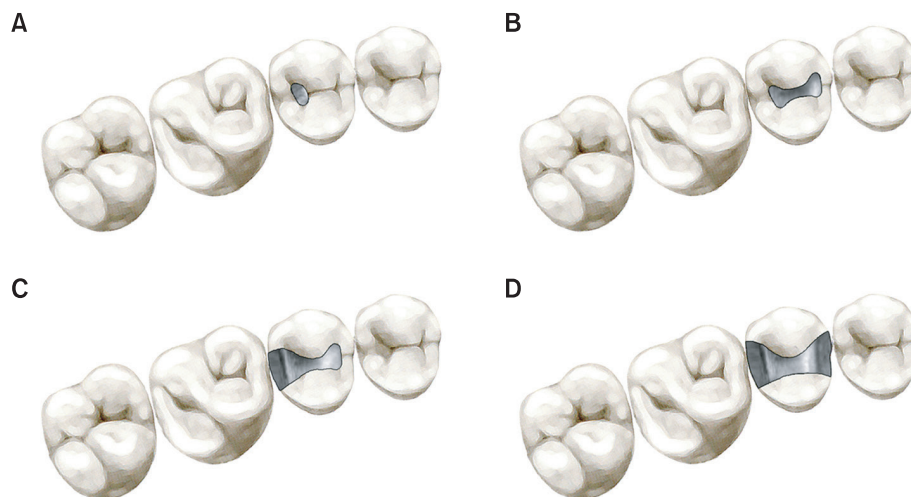


Figure 1. Illustration of the restorations. A, Small occlusal restoration; B, large occlusal restoration; C, disto-occlusal restoration; D, mesio-occluso-distal restoration.

For quantitative assessment, maximum linear discrepancy, area, and intensity of artifacts were measured. Maximum linear discrepancy was measured as the distance between shells at the most protruded point of the graphic (Figure 2A and 2B). Artifact area was defined as the area of discrepancy over 0.5 mm. The *shell/shell*

deviation function of the reverse engineering software was used to neglect discrepancies smaller than 0.5 mm. The graphics were exported to image analysis software (Image-Pro Plus 4.1; Media Cybernetics, Bethesda, MD, USA), and artifact area in the buccal, lingual, and occlusal views was measured by using the *area* function

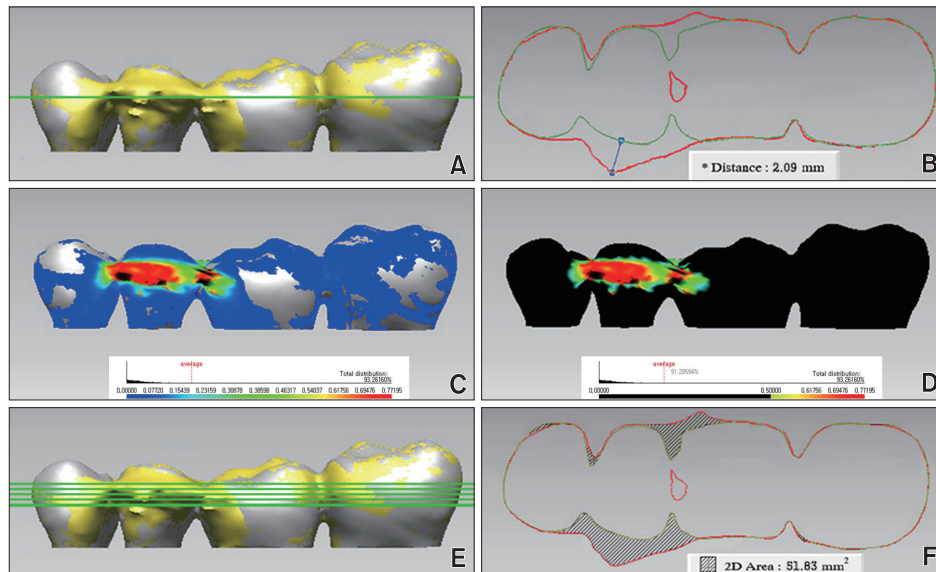


Figure 2. Quantitative assessment of artifacts on the basis of discrepancies of two models, each restoration model and no restoration model as the control. The present figures show the discrepancies between a mesio-occluso-distal restoration and the control. A and B, Maximum linear discrepancy was measured as the distance between the shells at the most protruded point of the graphic. C and D, Artifact area was defined as an area of discrepancy over 0.5 mm. E and F, Artifact intensity was defined as the sum of five discrepancy areas measured in cross-sectional graphics captured at the level of the maximum linear discrepancy and 0.5 and 1.0 mm above and below.

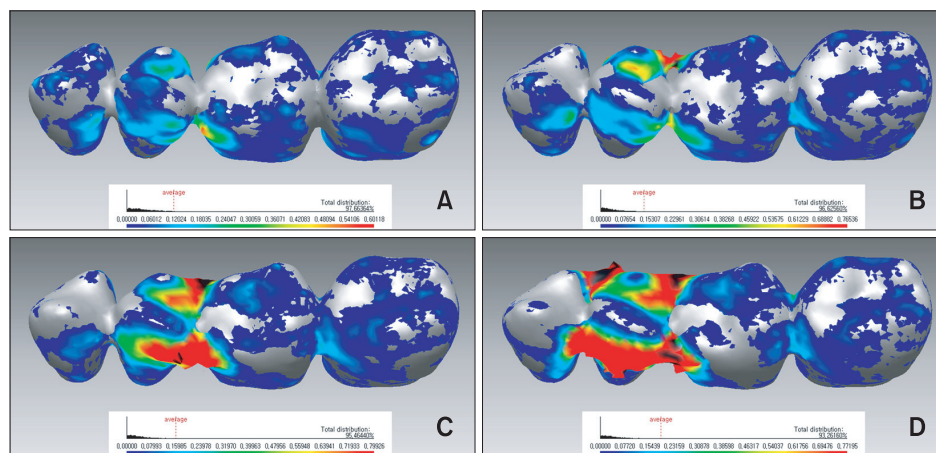


Figure 3. Color-mapped graphics obtained by registering three-dimensional surface models of the restorations with the control (no restoration). Discrepancies between the shells indicate artifacts due to amalgam restoration. Blue and red represent the minimum and maximum discrepancies, respectively. A, Small occlusal restoration; B, large occlusal restoration; C, disto-occlusal restoration; D, mesio-occluso-distal restoration.

of the software (Figure 2C and 2D). Artifact intensity was determined from cross-sectional views at the level of the maximum linear discrepancy and 0.5 and 1.0 mm above and below. The cross-sectional graphics were exported to the image analysis software, and the area of discrepancy at each level was measured. The sum of the five areas was defined as artifact intensity (Figure 2E and 2F).

Statistical analysis

Data were presented as means and standard deviations. One-way analysis of variance (ANOVA) was used to analyze parametric differences according to increasing restoration size, and the Tukey test was used for *post-hoc* comparisons. All analyses were carried out by the SPSS software program (version 18.0; SPSS Inc., Chicago, IL, USA).

RESULTS

Color mapping revealed artifacts in all cases. They were present not only on the second premolar but also

on the adjacent teeth and mostly on the buccal and lingual surfaces. On these surfaces, the artifacts showed a bridging pattern between the second premolar and the adjacent teeth. The extent of artifacts increased with increasing restoration size (Figure 3).

The maximum linear discrepancy was the least for the small occlusal restoration and the greatest for the mesio-occluso-distal restoration (Table 1), with significant differences among the models. Similarly, artifact area and intensity significantly increased with increasing restoration size (Tables 2 and 3, respectively).

DISCUSSION

A 3D surface model is influenced by several factors such as scan field and segmentation threshold value.²¹ This study used the specimen which consisted of extracted teeth. However, CBCT scans were performed in large FOV, 200 × 179 mm. It was because the FOV is commonly used for diagnosis of dentofacial deformities. We wanted to simulate CBCT scans of actual patient as much as possible while we used the specimen. The

Table 1. Maximum linear discrepancy according to restoration size (unit: mm)

	Small O restoration	Large O restoration	DO restoration	MOD restoration	Significance (p-value)
Maximum discrepancy	0.3 ± 0.2 ^a	0.6 ± 0.3 ^b	1.2 ± 0.3 ^c	2.1 ± 0.4 ^d	< 0.001

Values are presented as mean ± standard deviation. Different superscript letters indicate significant differences between groups. O, Occlusal; DO, disto-occlusal; MOD, mesio-occluso-distal.

Table 2. Artifact area according to restoration size (unit: mm²)

	Small O restoration	Large O restoration	DO restoration	MOD restoration	Significance (p-value)
Buccal	0.6 ± 1.1 ^a	5.2 ± 3.9 ^b	32.4 ± 9.5 ^c	48.3 ± 11.9 ^d	< 0.001
Lingual	1.2 ± 1.4 ^a	9.8 ± 6.1 ^b	29.4 ± 10.9 ^c	50.4 ± 12.8 ^d	< 0.001

Values are presented as mean ± standard deviation. Different superscript letters indicate significant differences between groups. O, Occlusal; DO, disto-occlusal; MOD, mesio-occluso-distal.

Table 3. Artifact intensity according to restoration size (unit: mm²)

	Small O restoration	Large O restoration	DO restoration	MOD restoration	Significance (p-value)
One level*	13.4 ± 5.9 ^a	20.3 ± 6.7 ^b	32.7 ± 5.6 ^c	51.8 ± 9.6 ^d	< 0.001
Five levels [†]	48.7 ± 19.9 ^a	82.2 ± 23.4 ^b	146.0 ± 23.8 ^c	234.4 ± 39.7 ^d	< 0.001

Values are presented as mean ± standard deviation. Different superscript letters indicate significant differences between groups. O, Occlusal; DO, disto-occlusal; MOD, mesio-occluso-distal.

*Discrepancy area measured at the level of the maximum linear discrepancy.

[†]Sum of the discrepancy areas measured at the level of the maximum linear discrepancy and 0.5 and 1.0 mm above and below.

segmentation threshold value also followed the default value of the program which is used as a routine in clinical practice.

Measurements of 3D surface models reconstructed from CBCT scan data are reportedly larger than physical measurements.²²⁻²⁴ Ye et al.²⁴ showed that volumetric measurements from CBCT scans are larger than those from laser scans of extracted human teeth. Laser-scanned images might be the gold standard for experiments with 3D surface models. However, CBCT scans without restoration were used as the control in this study because the aim was to assess artifacts from metallic restorations in CBCT scans. Comparison of the accuracy of 3D surface models derived from CBCT with those from other imaging methods was not the focus. After registering each restored model with the control model of a specimen, discrepancies between the shells were evaluated both graphically and numerically.

Color mapping revealed artifacts in all cases, including small occlusal restorations. They were present not only on the second premolar but also on the adjacent teeth. It is because dental amalgam is a highly absorbing material. It causes beam hardening artifacts which are the most prominent artifacts induced by high-density objects in the beam's path.^{11,12,25} In beam hardening, a polychromatic X-ray beam gradually becomes harder when passing through high-density objects, by which lesser-energy photons are absorbed and only higher-energy photons pass through. While the artifact appears as streaks in 2D images, it "bulges" in 3D surface models. In the case of the larger restorations in this study, the artifacts showed a bridging pattern across the second premolar and adjacent teeth. This finding suggests that metallic restorations strongly affect the quality of 3D CBCT reconstructions.

The finding of artifacts mostly on the buccal and lingual surfaces compared with the occlusal surface indicates that artifacts appear in the horizontal direction, not vertically, on 3D surface models. The difference is likely attributable to the direction of the X-ray beam of the scanner, because the emitter of a CBCT scanner rotates around an object in the horizontal direction.

In this study, the maximum linear discrepancy was the least and greatest in models of the small occlusal and mesio-occluso-distal restorations, respectively. Positive relationships between the extent of artifact and the restoration size were also observed in the artifact area and intensity measurements. While artifact reduction can be attempted by reconstruction algorithms,²⁶ a simple alternative is to replace the highly absorbing material with a less dense one, such as composite resin, before CBCT scanning. During orthodontic treatment, polycarbonate brackets are preferable to metallic brackets. The resulting changes in artifacts can be evaluated

quantitatively by the method used in this study.

Another way to avoid artifacts in 3D surface models of the head is to replace the artifact-laden dental part with optical or laser-scanned dental images. For fabricating appliances such as surgical splint and indirect bonding tray, the dental part should be replaced with images containing detailed occlusal and accurate interocclusal data. However, these procedures are complicated for practitioners, particularly when fiducial markers are used for registering models derived from two imaging modalities.^{13,15,27} A simpler method is to integrate the digital data of a plaster cast with CT data by surface registration^{13,16-18} using an iterative closest point algorithm,²⁰ without fiducial markers. However, it should be noted that artifacts affect registration accuracy in case of using surface registration in the implementation of digital dental model into CT scan data.^{18,28} Lin et al.¹⁸ reported greater registration errors in models with artifacts than in those without artifacts although all the measurements exhibited acceptable interoperator and intraoperator reproducibility.

In this study, CBCT images were obtained with a large FOV, so a large voxel size was used. As artifacts differ according to voxel size and FOV, it needs to be evaluated under other scan conditions, such as smaller voxel size. Further, comparative studies with other dental materials, such as composite resin, are needed, considering that beam hardening artifacts are influenced by object density. In particular, the 3D surface models created in this study do not represent actual patients. Future studies with orthodontic patients are needed.

CONCLUSION

Metallic restorations induce considerable artifacts in 3D dental surface models. Artifact reduction should be taken into consideration for a proper diagnosis and treatment planning when using 3D surface model derived by CBCT in dentofacial deformity patients. On the other hand, the present study would be useful for assessing various artifact-inducing factors, such as scan field, voxel size, segmentation threshold value, and dental material type.

REFERENCES

1. Hwang HS, Hwang CH, Lee KH, Kang BC. Maxillofacial 3-dimensional image analysis for the diagnosis of facial asymmetry. *Am J Orthod Dentofacial Orthop* 2006;130:779-85.
2. Terajima M, Nakasima A, Aoki Y, Goto TK, Tokumori K, Mori N, et al. A 3-dimensional method for analyzing the morphology of patients with maxillofacial deformities. *Am J Orthod Dentofacial*

- Orthop 2009;136:857-67.
3. Girod S, Keeve E, Girod B. Advances in interactive craniofacial surgery planning by 3D simulation and visualization. *Int J Oral Maxillofac Surg* 1995;24:120-5.
 4. Xia J, Ip HH, Samman N, Wang D, Kot CS, Yeung RW, et al. Computer-assisted three-dimensional surgical planning and simulation: 3D virtual osteotomy. *Int J Oral Maxillofac Surg* 2000;29:11-7.
 5. Xia JJ, Gateno J, Teichgraeber JF, Christensen AM, Lasky RE, Lemoine JJ, et al. Accuracy of the computer-aided surgical simulation (CASS) system in the treatment of patients with complex craniomaxillofacial deformity: A pilot study. *J Oral Maxillofac Surg* 2007;65:248-54.
 6. Gateno J, Xia JJ, Teichgraeber JF, Christensen AM, Lemoine JJ, Liebschner MA, et al. Clinical feasibility of computer-aided surgical simulation (CASS) in the treatment of complex cranio-maxillofacial deformities. *J Oral Maxillofac Surg* 2007;65:728-34.
 7. Schulze R, Heil U, Gross D, Bruellmann DD, Dranischnikow E, Schwanecke U, et al. Artefacts in CBCT: a review. *Dentomaxillofac Radiol* 2011; 40:265-73.
 8. Endo M, Tsunoo T, Nakamori N, Yoshida K. Effect of scattered radiation on image noise in cone beam CT. *Med Phys* 2001;28:469-74.
 9. Mozzo P, Procacci C, Tacconi A, Martini PT, Andreis IA. A new volumetric CT machine for dental imaging based on the cone-beam technique: preliminary results. *Eur Radiol* 1998;8:1558-64.
 10. Hsieh J, Molthen RC, Dawson CA, Johnson RH. An iterative approach to the beam hardening correction in cone beam CT. *Med Phys* 2000;27:23-9.
 11. De Man B, Nuyts J, Dupont P, Marchal G, Suetens P. Metal streak artifacts in x-ray computed tomography: a simulation study. *IEEE Trans Nucl Sci* 1999;46:691-6.
 12. De Man B, Nuyts J, Dupont P, Marchal G, Suetens P. Reduction of metal streak artefacts in X-ray computed tomography using a transmission maximum a posteriori algorithm. *IEEE Trans Nucl Sci* 2000; 47:977-81.
 13. Gateno J, Xia J, Teichgraeber JF, Rosen A. A new technique for the creation of a computerized composite skull model. *J Oral Maxillofac Surg* 2003; 61:222-7.
 14. Nkenke E, Zachow S, Benz M, Maier T, Veit K, Kramer M, et al. Fusion of computed tomography data and optical 3D images of the dentition for streak artefact correction in the simulation of orthognathic surgery. *Dentomaxillofac Radiol* 2004; 33:226-32.
 15. Uechi J, Okayama M, Shibata T, Muguruma T, Hayashi K, Endo K, et al. A novel method for the 3-dimensional simulation of orthognathic surgery by using a multimodal image-fusion technique. *Am J Orthod Dentofacial Orthop* 2006;130:786-98.
 16. Kim BC, Lee CE, Park W, Kang SH, Zhengguo P, Yi CK, et al. Integration accuracy of digital dental models and 3-dimensional computerized tomography images by sequential point- and surface-based markerless registration. *Oral Surg Oral Med Oral Pathol Oral Radiol Endod* 2010;110:370-8.
 17. Noh H, Nabha W, Cho JH, Hwang HS. Registration accuracy in the integration of laser-scanned dental images into maxillofacial cone-beam computed tomography images. *Am J Orthod Dentofacial Orthop* 2011;140:585-91.
 18. Lin HH, Chiang WC, Lo LJ, Sheng-Pin Hsu S, Wang CH, Wan SY. Artifact-resistant superimposition of digital dental models and cone-beam computed tomography images. *J Oral Maxillofac Surg* 2013;71: 1933-47.
 19. Lee WB, Theodore MR, Aldridge DW. Class I, II, and VI amalgam restorations. In: Herald OH, Edward JS, Andre VR, editors. *Sturdevant's art and science of operative dentistry*. 6th ed. St Louis: Mosby; 2012.
 20. Besl PJ, McKay ND. A method for registration for 3-D shapes. *IEEE Trans Patt Anal Machine Intell* 1992;14:239-56.
 21. Hassan B, Couto Souza P, Jacobs R, de Azambuja Berti S, van der Stelt P. Influence of scanning and reconstruction parameters on quality of three-dimensional surface models of the dental arches from cone beam computed tomography. *Clin Oral Investig* 2010;14:303-10.
 22. Coward TJ, Scott BJ, Watson RM, Richards R. A comparison between computerized tomography, magnetic resonance imaging, and laser scanning for capturing 3-dimensional data from an object of standard form. *Int J Prosthodont* 2005;18:405-13.
 23. Liang X, Lambrichts I, Sun Y, Denis K, Hassan B, Li L, et al. A comparative evaluation of cone beam computed tomography (CBCT) and multi-slice CT (MSCT). Part II: On 3D model accuracy. *Eur J Radiol* 2010;75:270-4.
 24. Ye N, Jian F, Xue J, Wang S, Liao L, Huang W, et al. Accuracy of in-vitro tooth volumetric measurements from cone-beam computed tomography. *Am J Orthod Dentofacial Orthop* 2012;142:879-87.
 25. Schulze RK, Berndt D, d'Hoedt B. On cone-beam computed tomography artifacts induced by titanium implants. *Clin Oral Implants Res* 2010;21:100-7.
 26. Zhang Y, Zhang L, Zhu XR, Lee AK, Chambers M, Dong L. Reducing metal artifacts in cone-beam CT images by preprocessing projection data. *Int J Radiat Oncol Biol Phys* 2007;67:924-32.

27. Swennen GR, Mommaerts MY, Abeloos J, De Clercq C, Lamoral P, Neyt N, et al. A cone-beam CT based technique to augment the 3D virtual skull model with a detailed dental surface. *Int J Oral Maxillofac Surg* 2009;38:48-57.
28. Biao Y. Registration accuracy according to the removal of artifact area in the integration of laser-scanned dental images into maxillofacial cone-beam CT images [Master's thesis]. Gwangju: Chonnam National University; 2012.